Supporting Information for

A Zn-S Aqueous Primary Battery with High Energy and Flat Discharge Plateau

Lian-Wei Luo,[a] Chong Zhang,[a,b,*] Xianyong Wu,[b] Changzhi Han,[a] Yunkai Xu,[b] Xiulei Ji,[b,*] Jia-Xing Jiang[a,*]

[a]Key Laboratory of Applied Surface and Colloid Chemistry (Shaanxi Normal University), Ministry of Education, Key Laboratory for Macromolecular Science of Shaanxi Province, Shaanxi Key Laboratory for Advanced Energy Devices, School of Materials Science and Engineering, Shaanxi Normal University, Xi'an 710062, P. R. China.
E-mail: chongzhangabc@snnu.edu.cn, jiaxing@snnu.edu.cn

[b]Department of Chemistry, Oregon State University, Corvallis, OR, 97331-4003, United States.
E-mail: david.ji@oregonstate.edu

Experimental Procedures

Materials: $ZnSO_4$, $Zn(OTF)_2$, $Zn(AC)_2$, $ZnCl_2$, Zn foil (0.1 mm thick), and commercial sulfur powder were purchased from Inno-chem or Adamas-beta Co. Ltd. Ketjen black (KB) were purchased from XFNANO Co. Ltd. Glass fiber (GF/D borosilicate) was purchased from Whatman. Carbon paper was purchased from Fuel Cell Store.

Preparation of sulfur/carbon composites: The sulfur/carbon composites were prepared by the reported melt-diffusion method.[1] Typically, 800 mg sulfur was first ground with 200 mg KB in a mortar for 30 minutes, and then the mixture was ball-milled for 5 hours at a rotating speed of 300 rpm. The composite was collected and pressed into a pellet, which was sealed in an autoclave and held at 155 °C for 6 hours.

Characterization: X-ray diffraction (XRD) patterns were collected on X-ray diffractometer (D/Max-3c). Nitrogen adsorption and desorption isotherms were collected on an ASAP 2420-4 (micromeritics) volumetric adsorption analyze at 77.3 K. The surface area was obtained in the relative pressure (P/P_o) of 0.05-1.0. The pore size distribution curve is obtained by NL-DFT using the adsorption branch isotherm. The sample was degassed under vacuum (10^{-5} bar) at 40 ^oC for 24 hours before analysis. The thermal performance of the KB-S composites was estimated using thermogravimetric analysis with a different thermal analysis apparatus (Q1000DSC+LNCS+FACS Q600DT) in the temperature range from 30 to 800 ^oC under nitrogen atmosphere with a heating rate

of 10 ^{o}C min^{-1}. The microscopic morphology of the mixture was studied on a field emission scanning electron microscope (SEM) (SU8020, Hitachi). Transmission electron microscopy (TEM) images and energy dispersive X-ray (EDX) spectra of the KB-S composites were recorded at JEM-2800 TEM/STEM.

Measurements of electrochemical performance: The cathode was prepared by the following method: the S-carbon nanocomposite cathode was mixed with KB and sodium alginate with a mass ratio of 7:2:1. Water was added into the above mixture as the solvent to form a slurry. Afterwards, the slurry was casted on a carbon paper current collector and then dried at room temperature. The galvanostatic charge/discharge performance of Zn-S battery was estimated in two-electrode cells, in which the S-carbon nanocomposite, 1 M Zn^{2+}-containing aqueous solution, and Zn foil were employed as the cathode, electrolyte, and anode, respectively. The electrochemical impedance spectra were obtained on a Gamry Interface 1010E workstation. The galvanostatic charge/discharge measurements were studied on an LANHE CT2001A battery tester.

The Warburg coefficient σ can be calculated from the following equation:

$$Z_{re} = R_e + R_{ct} + \sigma\omega^{-0.5} \quad (1)$$

Where R_e is the electrolyte resistance, R_{ct} is the charge transfer resistance, ω is the angular frequency in the low frequency region, Z_{re} is the real axis resistance in the low frequency region; Thus, the Warburg coefficient σ is the slope of the plot Z_{re} vs $\omega^{-0.5}$, as shown in the following **Fig. S11**.

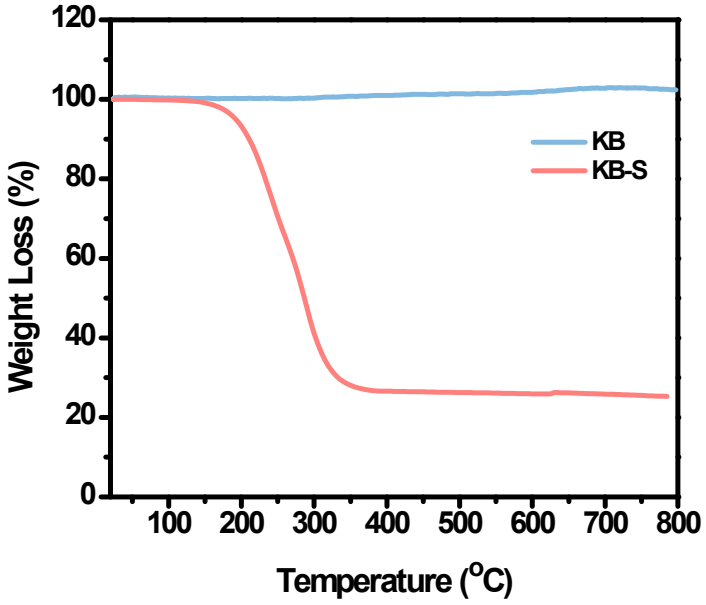

Fig. S1 The TGA curves for KB and KB-S.

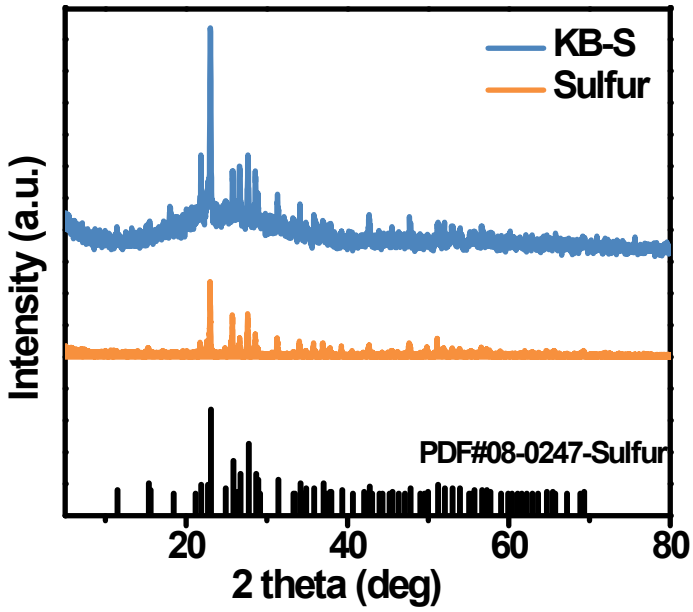

Fig. S2 The XRD patterns for sulfur and KB-S.

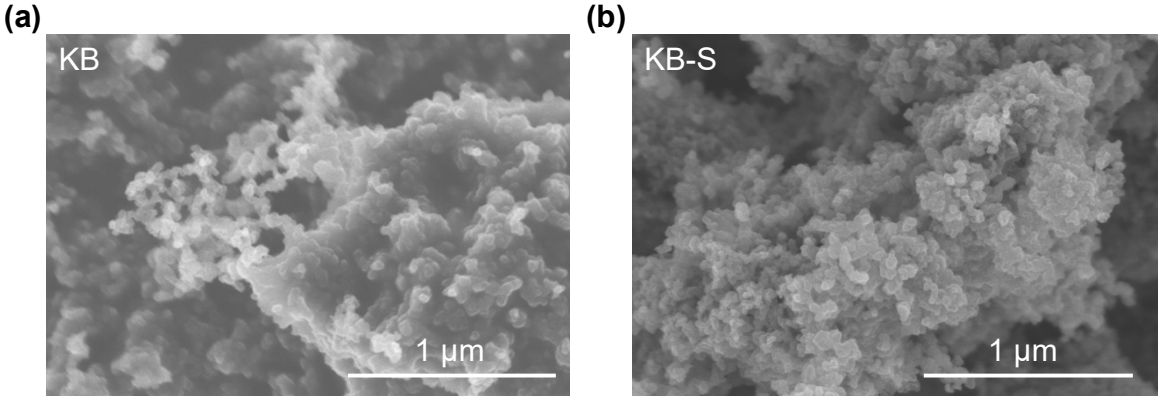

Fig. S3 The SEM images of KB and KB-S.

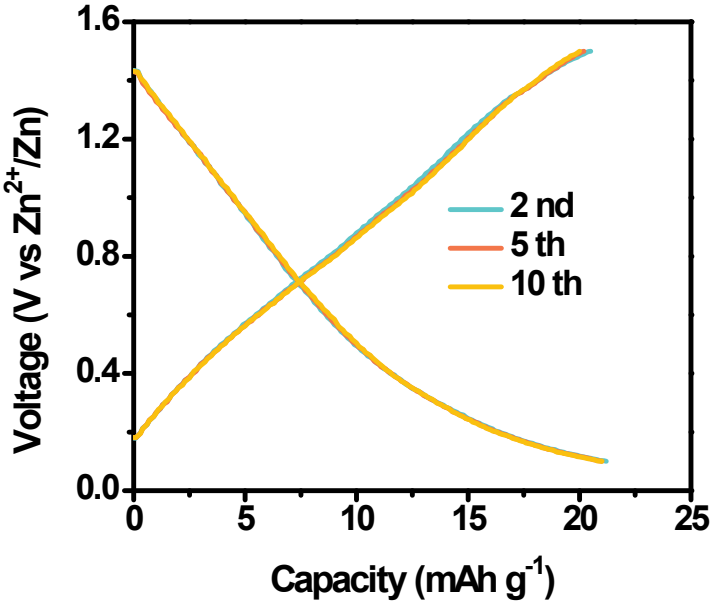

Fig. S4 The GCD profiles of Ketjen black at 50 mA g^{-1}.

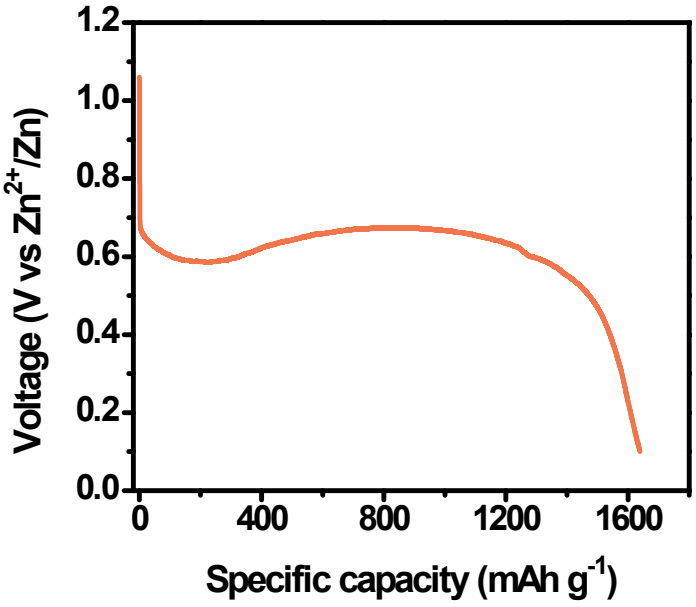

Fig. S5 The discharge profile of aqueous Zn-S full cell, in which the mass ratio of Zn to sulfur is 2.2:1. The specific capacity was calculated based on the mass of sulfur.

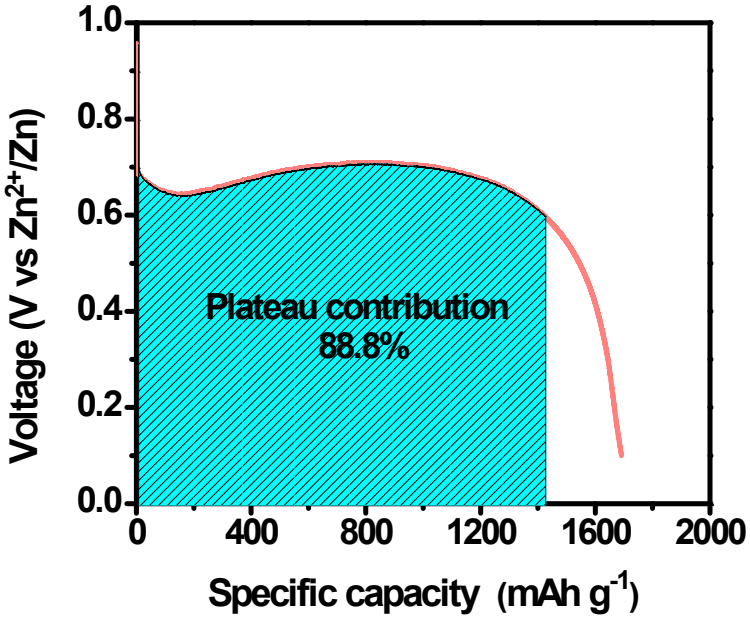

Fig. S6 The plateau contribution for the total energy density.

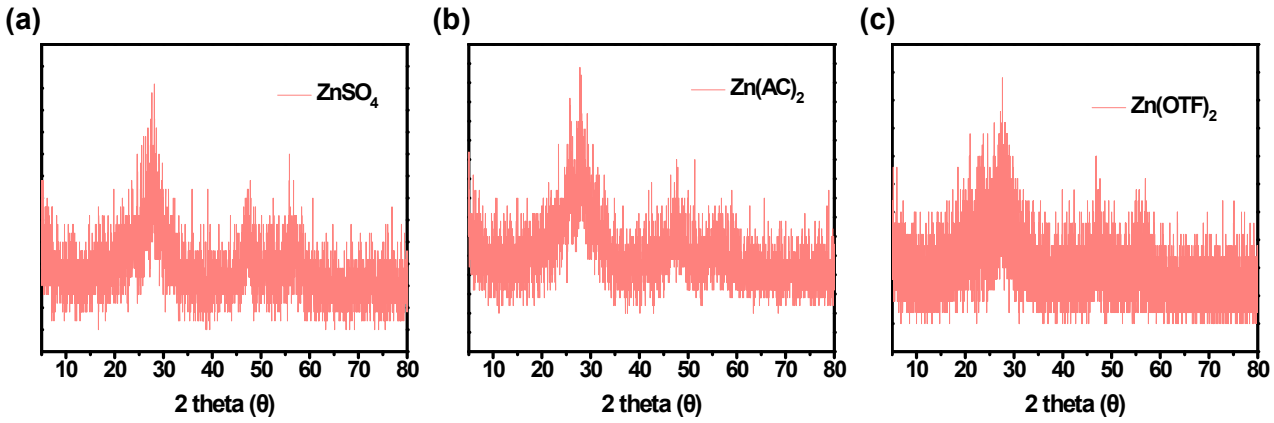

Fig. S7 The *ex-situ* XRD patterns of the discharged KB-S cathode working with different electrolytes at 50 mA g^{-1}.

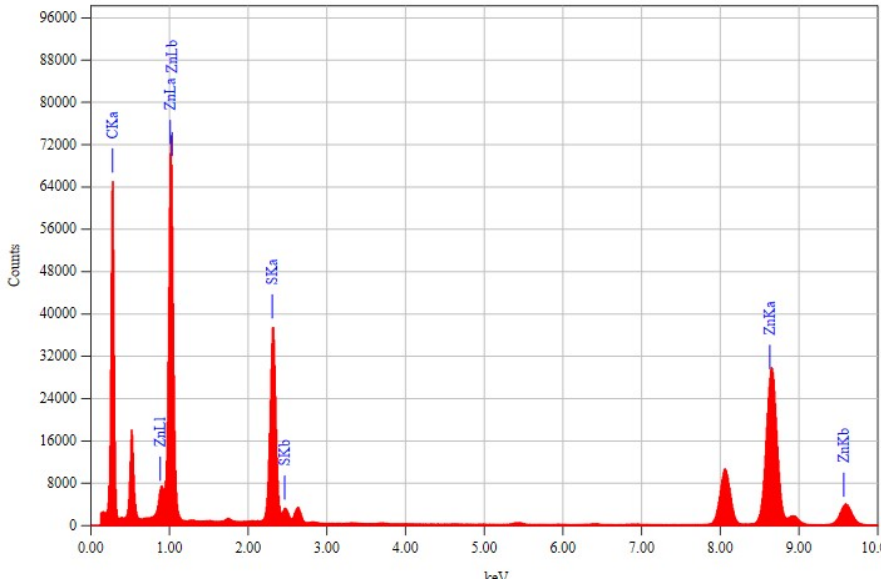

Fig. S8 The EDX spectrum of the discharged cathode.

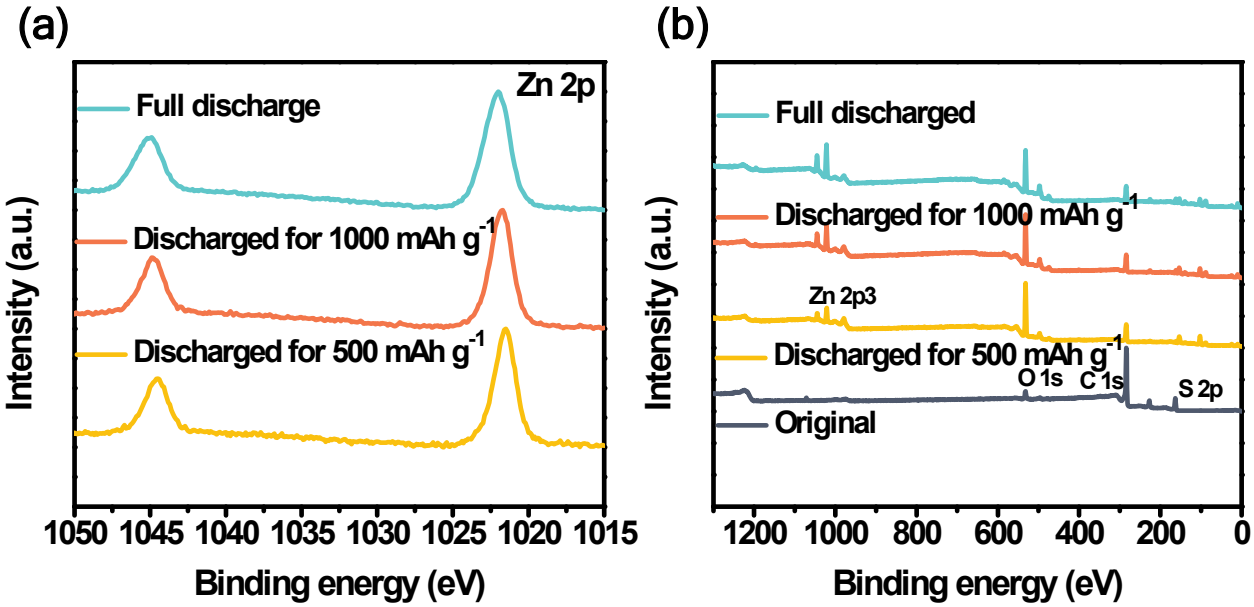

Fig. S9 (a) The XPS spectra of Zn 2p at different states of discharge. (b) The XPS survey spectra of the KB-S cathodes at different states of discharge.

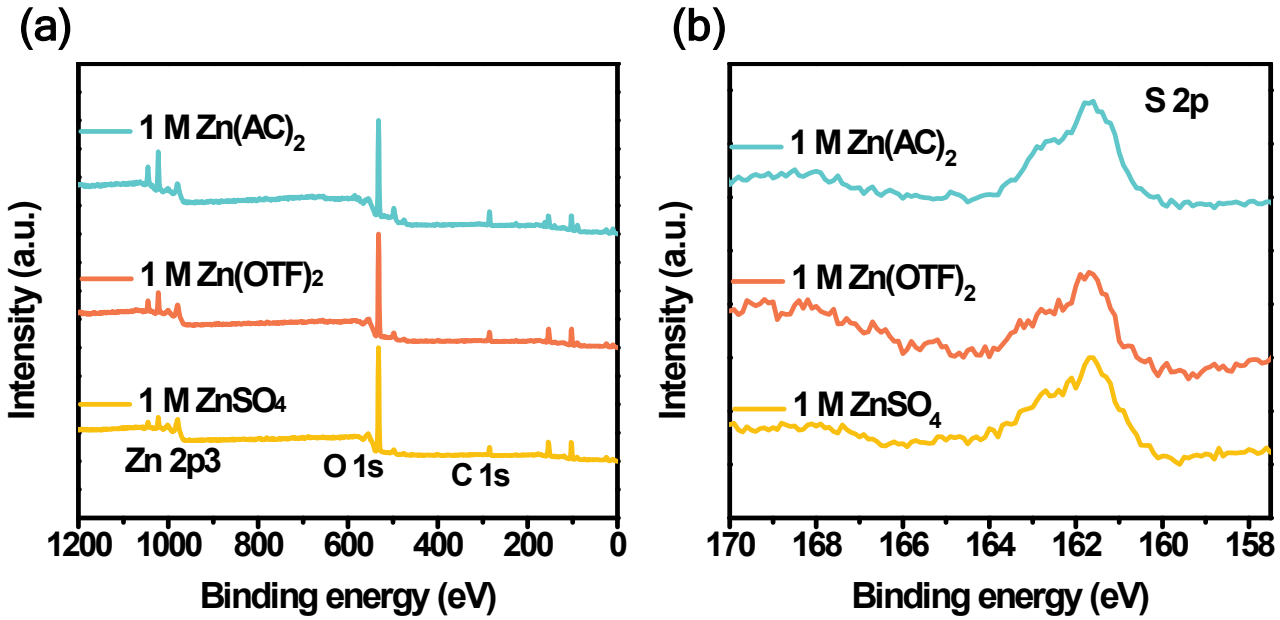

Fig. S10 (a) The XPS survey spectra of the KB-S electrodes working in different electrolytes. (b) The XPS spectra of S 2p from the KB-S cathodes worked in different electrolytes.

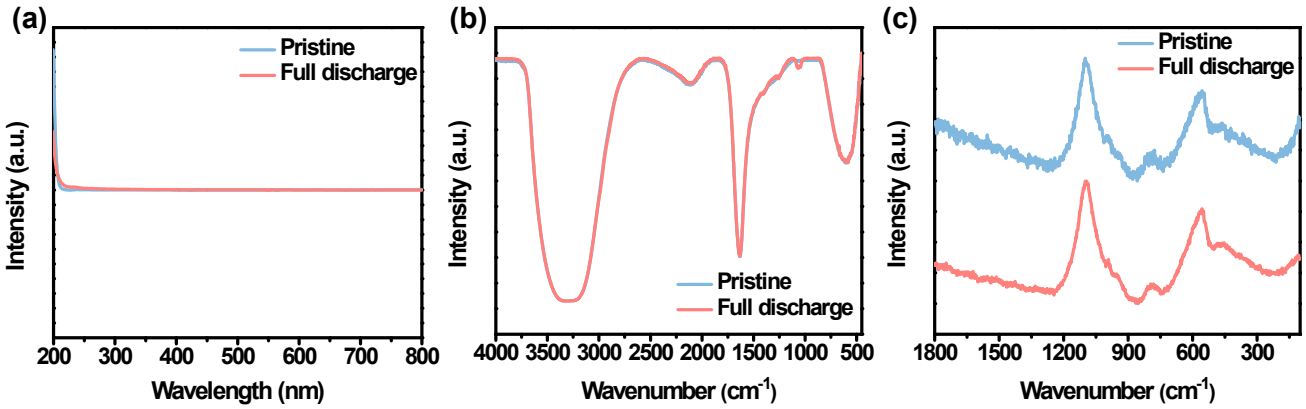

Fig. S11 The characterization of the electrolytes before and after the discharge process. (a) The UV-Vis absorption spectra. (b) The FT-IR spectra. (c) The Raman spectra.

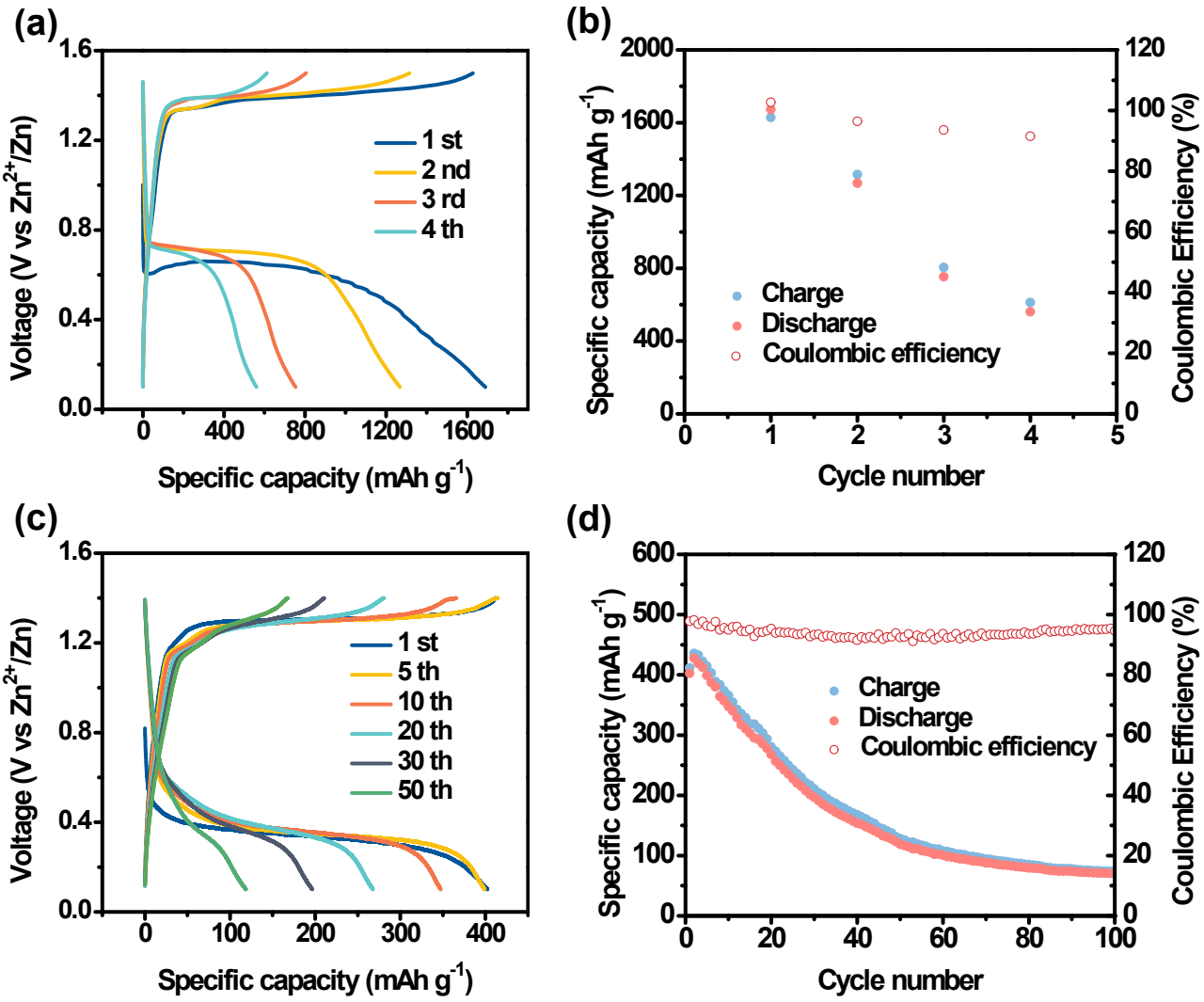

Fig. S12 The electrochemical performance of Zn-S battery using $ZnCl_2$ electrolytes with different concentrations. (a) GCD curves and (b) cycling performance in 1 M $ZnCl_2$ electrolyte. (c) GCD curves and (d) cycling performance in 30 m $ZnCl_2$ electrolyte.

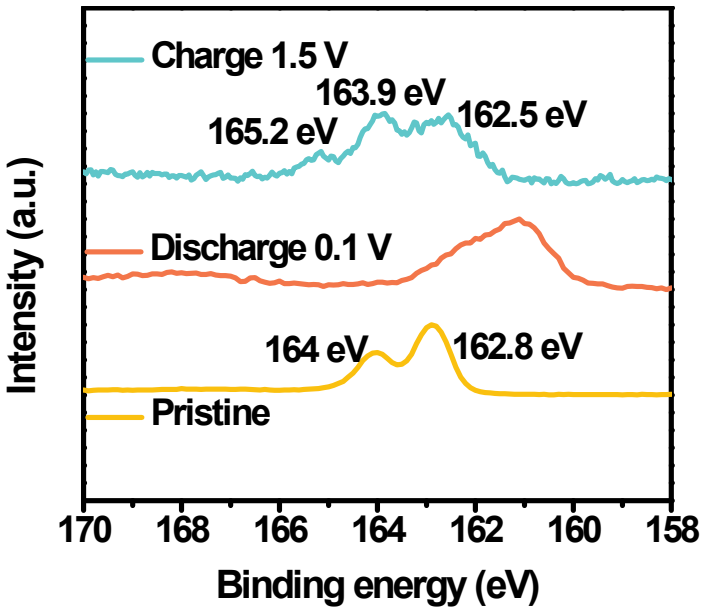

Fig. S13 The XPS spectra of S 2p from the KB-S cathodes at different states of charge. After charging the battery to 1.5 V, a new peak emerged at around 165.2 eV, which could be attributed to the S-O species from sulfate.[2,3]

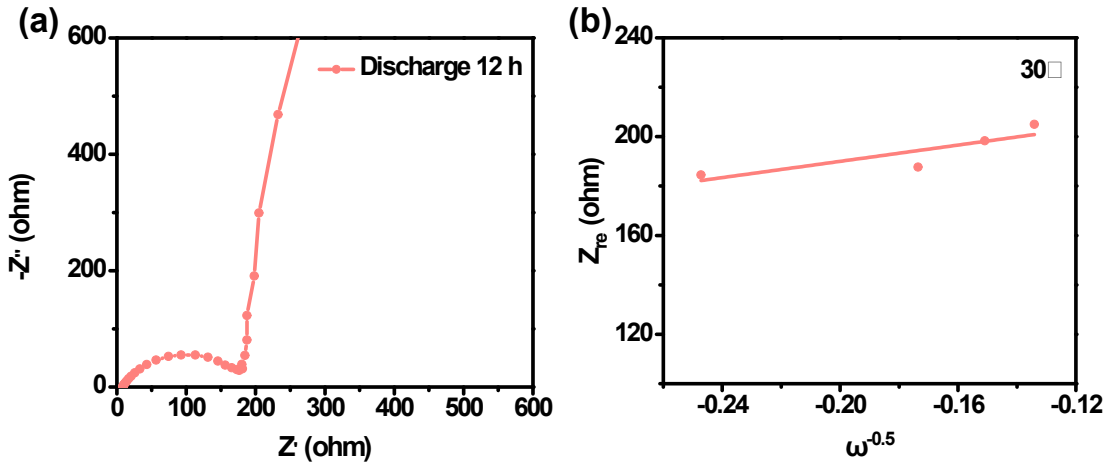

Fig. S14 (a) The Nyquist plot of the Zn-S cell after discharging for 12 h. (b) The plots of Z_{re} vs $\omega^{-0.5}$.

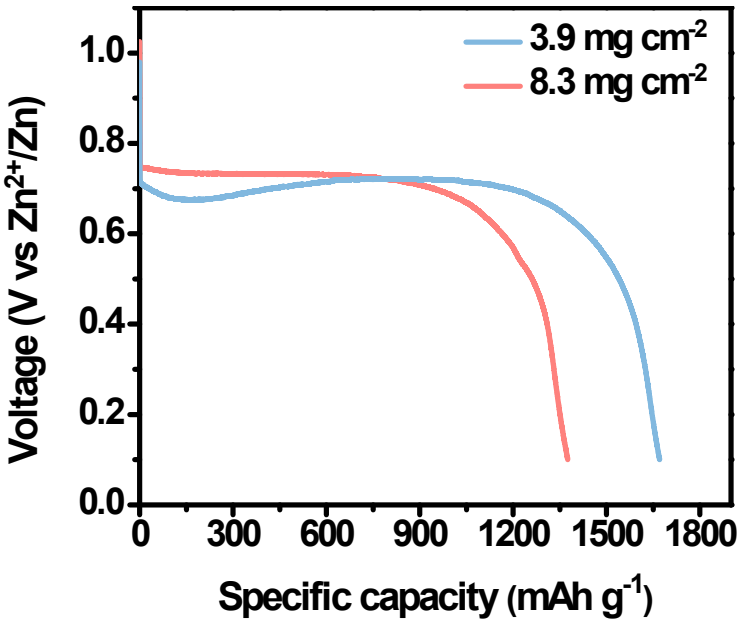

Fig. S15 The discharge curves of the KB-S cathodes with different sulfur loading of 3.9 and 8.3 mg cm^{-2}.

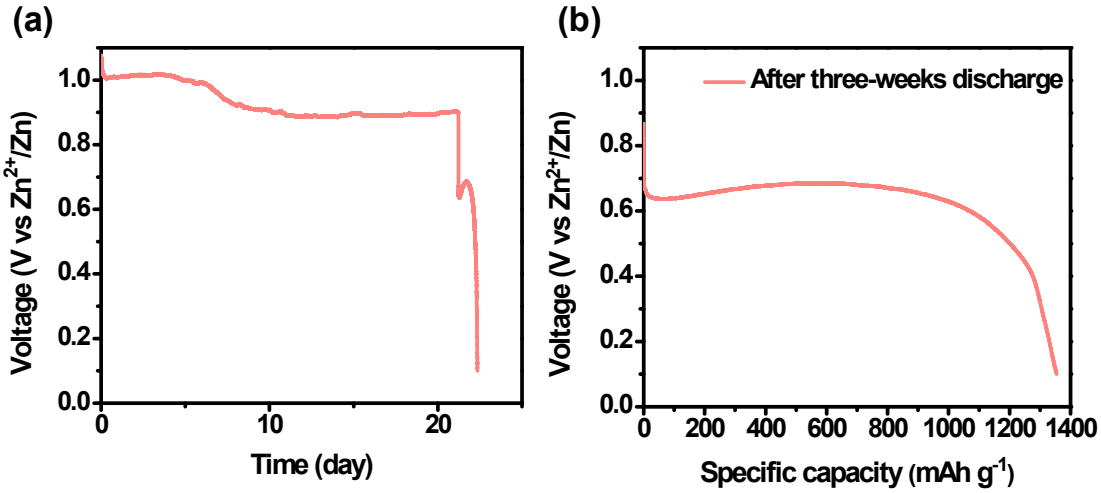

Fig. S16 The self-discharge behavior of Zn-S batteries. (a) The open circuit potential during self-discharge measurement. (b) The discharge curve after resting the battery for 21 days.

Table S1. The summary of electrochemical performance for recent primary batteries.

Cathode materials	Anode materials	Electrolytes	Voltage (V)	Specific capacity (mAh g^{-1})	Specific energy (Wh kg^{-1})	Mass loading (mg cm^{-2})	Areal capacity (mAh cm^{-2})	Areal energy (mWh cm^{-2})	Ref.
MnO_2	Li	$LiClO_4$ in PC	2.31	130	300	-	-	-	4
CF_x	Li	1 M $LiClO_4$ in PC/DME/DOL	2.6	865	2180	1.33	1.15	2.9	5
AQ	Li	1 m LiTFSI DME with FEC	2.4	575	1300	0.6	0.345	0.78	6
Air	$FeSi_2$	0.5 M H_2SO_4	0.6-0.7	1900	1235	-	-	-	7
DDQ	Fe	14 M or 12 M methanesulfonic acid solution	0.85	69.4	59	2	0.139	0.118	8
MKB-S	Li	1.5 M LiTFSI in DME/DOL	~2.1	1310	2751	14	18.34	38.5	9
MnO_2	Zn	8.3 M KOH with 2.1 wt% gelling agents	~1.2	308	~370	-	-	-	10
KB-S	Zn	1 M $ZnCl_2$	~0.7	1683	1083.3	8.3	11.4	7.67	This work

Supplementary References

1. J. Wang, J. Yang, C. Wan, K. Du, J. Xie and N. Xu, *Adv. Funct. Mater.*, 2003, 13, 487-492.
2. Q. Pang, D. Kundu, M. Cuisinier and L. F. Nazar, *Nat. Commun.*, 2014, 5, 4759.
3. G. Zhou, L.-C. Yin, D.-W. Wang, L. Li, S. Pei, I. R. Gentle, F. Li and H.-M. Cheng, *ACS Nano*, 2013, 7, 5367-5375.
4. Y. Manane and R. Yazami, *J. Power Sources*, 2017, 359, 422-426.
5. Y. Li, X. Wu, C. Liu, S. Wang, P. Zhou, T. Zhou, Z. Miao, W. Xing, S. Zhuo and J. Zhou, *J. Mater. Chem. A*, 2019, 7, 7128-7137.
6. P. Sun, P. Bai, Z. Chen, H. Su, J. Yang, K. Xu and Y. Xu, *Small*, 2020, 16, 1906462.
7. J. Wang, L. Cui, S. Li, T. Pu, X. Fang, S. Kang and X. Zhang, *New J. Chem.*, 2020, 44, 1624-1631.

8. J. N. Ramavath, C. Ramachandra and K. Ramanujam, *ChemistrySelect*, 2018, 3, 10281-10286.

9. Y. Ma, H. Zhang, B. Wu, M. Wang, X. Li and H. Zhang, *Sci. Rep.*, 2015, 5, 14949.

10. J. W. Gallaway, M. Menard, B. Hertzberg, Z. Zhong, M. Croft, L. A. Sviridov, D. E. Turney,S. Banerjee, D. A. Steingart and C. K. Erdonmez, *J. Electrochem. Soc.*, 2014, 162, A162-A168.